

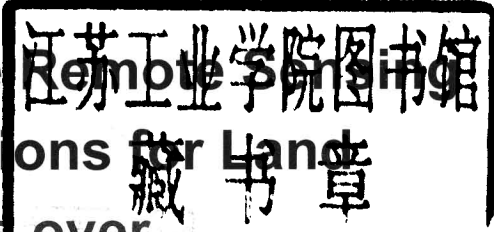
Combining Satellite Remote Sensing with Field Observations for Land Surface Heat Fluxes over Inhomogeneous Landscape

MA Yaoming, Osamu TSUKAMOTO

China Meteorological Press

Funded by the Innovation Project of Cold and Arid Regions Environmental and Engineering Research Institute,Chinese Academy of Sciences (Grant No.CACX210072),Chinese National Key Project (Grant No.G1998040900),the Key Project of the Chinese Academy of Sciences (KZCX2-301), the “GEWEX Asian Monsoon Experiment on Tibetan Plateau (GAME/Tibet)” Project , and the Project of National Natural Science Foundation of China “HEIhe basin Field Experiment (HEIFE)”

Combining Satellite Remote Sensing
with Field Observations for Land
Surface Heat Fluxes over
Inhomogeneous Landscape



MA Yaoming, Osamu TSUKAMOTO

China Meteorological Press

Copyright © 2002 by China Meteorological Press
Published by China Meteorological Press
Printed in Beijing

All rights reserved. No part of this publication may be reproduced, stored in a retrieval system, or transmitted in any form or by any means, electronic, mechanical, photocopying, recording or otherwise, without the permission of the copyright owner.

First published in June 2002

China Meteorological Press Foreign Language Book No. 131

ISBN 7-5029-3399-9

卫星遥感和野外观测联合测定
不均匀地面上的热通量

责任编辑：张斌 终审：周诗健

气象出版社 出版发行

(北京市海淀区中关村南大街 46 号 100081)

* * *

开本：787×960 1/16 印张：12 字数：300 千字

2002 年 7 月第一版 2002 年 7 月第一次印刷

ISBN 7-5029-3399-9/P·1207

定价：50.00 元

parameterization methods are better approaches to get related air-land parameters over inhomogeneous landscape.

The utilization field of the new remote sensing parameterization methods and the recommendations of improving the scheme have also been presented in this book.

Key words: satellite remote sensing, field observations, land surface variables, vegetation variables, land surface heat fluxes, validation, inhomogeneous landscape, GAME/Tibet, HEIFE, AECMP'95, NOAA AVHRR, Landsat TM

Preface

The work reported in this book was funded by the Innovation Project of Cold and Arid Regions Environmental and Engineering Research Institute, Chinese Academy of Sciences (Grant No. CACX210072), Chinese National Key Project (Grant No.G1998040900), the Key Project of the Chinese Academy of Sciences (KZCX2-301), the “GEWEX Asian Monsoon Experiment on Tibetan Plateau (GAME/Tibet) ” project and “HEIhe basin Field Experiment (HEIFE)” project. The idea about this research was formed after the HEIFE project experiment in 1995 and was strengthened during the Intensive Observational Period (IOP) of GAME/Tibet.

We wish to express our sincere thanks to Profs. Massimo Menenti (Universite Louis Pasteur–Strasbourg), WANG Jiemin (Cold and Arid Regions Environmental and Engineering Research Institute, Chinese Academy of Sciences), Hirohiko Ishikawa (Kyoto University), Toshio Koike (University of Tokyo), Tetsuzo Yasunari (Tsukuba University), R.A.Feddes (Wageningen UR), Toshihiko Maitani (Okayama University), Eiji Ohtaki (Okayama University), YAO Tandong (Cold and Arid Regions Environmental and Engineering Research Institute, Chinese Academy of Sciences), LU Shihua (Cold and Arid Regions Environmental and Engineering Research Institute, Chinese Academy of Sciences), LIU Xinsheng (Cold and Arid Regions Environmental and Engineering Research Institute, Chinese Academy of Sciences), Ken Sahashi (Okayama University), Ichiro Tamagawa (Gifu University), HUANG Ronghui (Institute of Atmospheric Physics, Chinese Academy of Sciences), DONG Wenjie (Institute of Atmospheric Physics, Chinese Academy of Sciences), Kenji Nakamura (Nagoya University) and Joon Kim (Yonsei University) for many very useful discussions, good suggestions and supports during the field experiments of HEIFE , GAME/Tibet and the data analysis. We can finish this book due to their very kindly help and encouragement.

We are indebted to Dr. SU Zhongbo (Alterra Green World Research, Wageningen UR), Dr. LI Zhaoliang (Universite Louis Pasteur – Strasbourg), Dr. Ken'ichi Ueno (University of Shiga Prefecture), Dr. Masayasu Hayashi and Dr. Minoru Gamo (National Institute of Resources and Environment), Dr. Henk Pelgrum (European Space Agency), Mr. Gerbert Roerink (Alterra Green World Research, Wageningen UR), Dr. WEN Jun, Dr.

YU Qihao, Dr. HU Zeyong, Dr. LI Jia, and Dr. GAO Feng (Cold and Arid Regions Environmental and Engineering Research Institute, Chinese Academy of Sciences) for their deep discussion and very kindly help in the satellite data processing and field data analysis.

We also express our very deep thanks to all the participants, who come from China, Japan and Korea in the field experiments of HEIFE, GAME/Tibet and AECMP'95 for their very hard work in the field.

We acknowledge all the scientists at the Institute for Hydrological-Atmospheric Sciences of Nagoya University, the scientists at the Satellite Earth Observation Group of Alterra Green World Research, Wageningen UR, the scientists at the Disaster Prevention Research Institute, Kyoto University and the colleagues at Cold and Arid Regions Environmental and Engineering Research Institute, Chinese Academy of Sciences.

Finally, special thanks to MA Yaoming's wife HAN Rong and Osamu Tsukamoto's wife Atsuko Tsukamoto for their understandings and supports on our fieldwork and research work for many years. Their hard work for our families led to this book finishing smoothly. Thanks are also given to our parents for their understandings and moral supports.

MA Yaoming (马耀明)

Osamu Tsukamoto (塚本修)

March 2002

Lanzhou, China

List of symbols

Symbol	Interpretation	Unit
C_D	Drag coefficient	-
C_H	Bulk transfer coefficient of sensible heat	-
c_s	Soil specific heat	$\text{J kg}^{-1} \text{K}^{-1}$
c_p	Air specific heat at constant pressure	$\text{J kg}^{-1} \text{K}^{-1}$
d_0	Zero-plane displacement	m
d_s	Earth-Sun distance	AU
E	Evaporation flux	$\text{kg m}^{-2} \text{s}^{-1}$
G	Acceleration due to gravity	m s^{-2}
G_0	Soil heat flux	W m^{-2}
h	Vegetation height	m
H	Sensible heat flux	W m^{-2}
k	Von Karman constant	-
kB^{-1}	Excess resistance to heat transfer	-
K^*	Net short-wave radiation flux	W m^{-2}
$K\downarrow$	Incoming short-wave radiation flux	W m^{-2}
$K\downarrow_{exo(b)}$	Mean in-band solar exo-atmospheric irradiance	W m^{-2}
$K\downarrow_{TOA}$	Radiation flux perpendicular to the top of atmosphere	W m^{-2}
$K\uparrow$	Outgoing short-wave radiation flux	W m^{-2}
L	Monin Obukhov stability length	m
$L\downarrow$	Incoming Long-wave radiation flux	W m^{-2}
$L\uparrow$	Outgoing Long-wave radiation flux	W m^{-2}
LAI	Leaf area Index	$\text{m}^2 \text{m}^{-2}$
$L_s(x,y)$	Satellite sensor detected radiance	W m^{-2}
$NDVI$	Normalized Difference Vegetation Index	-
$MSAVI$	Modified soil adjusted vegetation index	-
$NDVI_{max}$	Maximum NDVI	-
$NDVI_{min}$	Minimum NDVI	-
p	Pressure	Pa
q	Specific humidity	kg kg^{-1}
r_0	Surface reflectance (surface albedo)	-
r_a	Aerodynamic resistance	St m^{-1}
R_i	Richardson number	-

(continued)

Symbol	Interpretation	Unit
R_n	Net radiation flux	W m^{-2}
r_{sh}	Soil heat transportation resistance	St m^{-1}
$SAVI$	Soil adjusted vegetation index	-
t	Time	s
T	Temperature	K
T_4	Brightness temperature of channel 4 of NOAA/AVHRR	K
T_5	Brightness temperature of channel 5 of NOAA/AVHRR	K
T_{air-B}	Air temperature at the blending height	K
T_{sfc}	Surface temperature	K
T_a	Air temperature	K
T_B	Brightness temperature	K
u	Horizontal component of wind speed	m s^{-1}
U_*	Friction velocity	m s^{-1}
u_B	Wind speed at the blending height	m s^{-1}
W	Water vapor content	g m^{-3}
z	Reference height	m
z_{oh}	Thermodynamic roughness length	m
z_{om}	Aerodynamic roughness length	m
Z_{om}	Effective aerodynamic roughness length	m
z_B	Blending height	m
Z_{ref}	Reference height	m
ε_0	Surface emissivity	-
ε_4	Spectral emissivity of channel 4 on NOAA AVHRR	-
ε_5	Spectral emissivity of channel 5 on NOAA AVHRR	-
ζ	Monin-Obukhov stability correction parameter	-
θ	View angle of satellite	degree
θ_{sun}	Sun zenith angle	rad
λ	Wavelength	μm
λ	Latent heat of vaporization	J kg^{-1}
λE	Latent heat flux	W m^{-2}

(continued)

Symbol	Interpretation	Unit
Λ	Evaporation fraction	-
ρ	Air density	kg m^{-3}
ρ_s	Soil bulk density	kg m^{-3}
$\rho_s C_s$	Soil heat capacity	$\text{J m}^{-3} \text{K}^{-1}$
ρC_p	Air heat capacity	$\text{J m}^{-3} \text{K}^{-1}$
σ	Stefan Boltzmann constant	$\text{W m}^{-2} \text{K}^{-4}$
τ	Momentum flux	N m^{-2}
τ	Band average transmittance	-
τ_{sw}	Atmospheric short-wave transmittance	-
τ_λ	Spectral atmospheric transmittance	-
ϕ_m	Monin-Obukhov function for atmospheric momentum transport	-
ϕ_h	Monin-Obukhov function for atmospheric heat transport	-
ψ_{su}	Azimuth angle	rad
ψ_h	Stability correction for atmospheric heat transport	-
β	Scattering coefficient	-
β_0	Single scattering coefficient	-
ψ_m	Stability correction for atmospheric heat transport	-
δ	Solar declination	rad
$\omega(x)$	Solar angle hour	rad

List of acronyms

ABL	Atmospheric Boundary Layer
AECMP'95	Arid Experiment Comprehensive Monitoring Plan '95
AVHRR	Advanced Very High Resolution Radiometer
BST	Beijing Standard Time
CAREERI	Cold and Arid Regions Environmental and Engineering Research Institute
CAS	Chinese Academy of Sciences
DN	Digital Number
EFEDA	Echival First field Experiment in Desertification threatened Area
ET	Evapotranspiration
FIFE	First ISLSCP Field Experiment
GAME	GEWEX Asian Monsoon Experiment
GAME/Tibet	GEWEX Asian Monsoon Experiment on Tibetan Plateau
GEWEX	Global Energy and Water Cycle Experiment
GMT	Greenwich Mean Time
HAPEX	Hydrological and Atmospheric pilot Experiments
HEIFE	HEIhe basin Field Experiment
IAHS	International Association for Hydrological Sciences
IOP	Intensive Observational Period
ISLSCP	International Satellite Land Surface Climatological Project
LAI	Leaf Area Index
LIPAP	Lanzhou Institute of Plateau Atmospheric Physics
LST	Land Surface Temperature
LT	Local Time
MSAVI	Modified Soil Adjusted Vegetation Index
NDVI	Normalized Difference Vegetation Index
NIR	Near-InfraRed
NOAA	National Oceanic and Atmospheric Administration
PBL	Planetary Boundary Layer
SEBAL	Surface Energy Balance Algorithm for Land

SEBI	Surface Energy Balance Index
SVAT	Soil Vegetation Atmosphere Transfer
TIR	Thermal-InfraRed
TM	Thematic Mapper
TOA	Top of Atmosphere
VIS	Visible
UTM:	Universal Transfer Mercator
WCRP:	World Climate Research Plan
WMO:	World Meteorological Organization

Table of Contents

Abstract.....	(i)
Preface	(iii)
List of symbols	(v)
List of acronyms	(viii)
List of tables	(x)
List of figures.....	(xi)

Chapter 1 Introduction

1.1 Background	3
1.2 Objectives	6
1.3 Outline of the book	7

Chapter 2 Land surface process experiments: GAME/Tibet, HEIFE and AECMP'95

2.1 GAME/Tibet.....	11
2.2 HEIFE	15
2.3 AECMP'95	18

Chapter 3 Characteristics of energy transfer and micrometeorology in the atmospheric surface layer of GAME/Tibet, HEIFE and AECMP'95

3.1 Introduction	23
3.2 Experiments	23
3.2.1 Experiment of GAME/Tibet	23
3.2.2 Experiment of HEIFE	24
3.2.3 Experiment of AECMP'95	26
3.3 Data processing.....	26
3.3.1 The eddy correlation methodology	26
3.3.2 The Bowen ratio methodology	27
3.4 Results analysis	27
3.4.1 Land surface radiation balance	28
3.4.2 Land surface energy balance.....	31
3.4.3 Land surface heating field	34
3.4.4 Aerodynamic roughness length z_{om} and thermodynamic roughness length z_{oh} ..	35

3.4.4.1	An independent method of using a single sonic anemometer-thermometer	35
3.4.4.2	The profile method	35
3.4.4.3	Thermodynamic roughness length z_{oh}	38
3.4.5	Excess resistance to heat transfer kB'	39
3.5	Concluding remarks	45

Chapter 4 Determination of the regional land surface heat fluxes over inhomogeneous landscape of GAME/Tibet by combining NOAA/ AVHRR data with field observations

4.1	Introduction	49
4.2	Satellite data and field data	49
4.3	Vegetation variables	50
4.3.1	<i>NDVI</i>	50
4.3.2	Vegetation coverage P_v	51
4.3.3	Modified Soil Adjusted Vegetation Index <i>MSAVI</i>	52
4.3.4	Leaf area index <i>LAI</i>	52
4.4	Land surface variables	56
4.4.1	Surface reflectance (surface albedo)	56
4.4.2	Surface temperature	58
4.4.3	Relationship between surface reflectance and surface temperature	60
4.4.4	Surface emissivity	61
4.5	Parameterization of the regional land surface heat fluxes	63
4.5.1	Net radiation flux	63
4.5.2	Soil heat flux	64
4.5.3	Sensible heat flux	66
4.5.4	Latent heat flux	74
4.6	Case studies and validations	74
4.7	Concluding remarks	77

Chapter 5 Determination of the regional land surface heat fluxes over inhomogeneous landscape of HEIFE using Surface Energy Balance Algorithms for Land (SEBAL)

5.1	Introduction	83
5.2	Satellite data and field data	83
5.3	Land surface variables and <i>NDVI</i>	84

5.3.1	Surface reflectance $r_0(x,y)$	84
5.3.2	$NDVI(x,y)$	87
5.3.3	Land surface emissivity $\varepsilon_0(x,y)$	88
5.3.4	Land surface temperature $T_{sfc}(x,y)$	88
5.3.5	Relationship between surface reflectance and surface temperature	90
5.4	Parameterization of the regional land surface heat fluxes	91
5.4.1	Net radiation flux $R_n(x,y)$	91
5.4.2	Soil heat flux $G_0(x,y)$	91
5.4.3	Sensible heat flux $H(x,y)$	93
5.4.4	Latent heat flux $\lambda E(x,y)$	96
5.4.5	Case study	96
5.4.5.1	The distribution of surface variables and $NDVI$	96
5.4.5.2	The distribution of pixel-wise land surface energy fluxes	99
5.4.6	Validation of the calculated results	102
5.5	Concluding remarks	103

Chapter 6 Parameterization of the regional land surface heat fluxes over inhomogeneous landscape of HEIFE and AECMP'95 by combining Landsat TM data with field observations

6.1	Introduction	107
6.2	Landsat TM data and field observation data	107
6.3	Theory and scheme	108
6.3.1	Land surface variables	109
6.3.1.1	Surface reflectance	109
6.3.1.2	Surface temperature	112
6.3.2	Vegetation variables	113
6.3.3	Determination of the regional land surface heat fluxes	114
6.3.3.1	Net radiation flux	114
6.3.3.2	Soil heat flux	114
6.3.3.3	Sensible heat flux	115
6.3.3.4	Latent heat flux	120
6.4	Case study and validation	120
6.5	Concluding remarks	123

Chapter 7 Summary and conclusions	133
References.....	155
Curriculum Vitae.....	171

Abstract

Arid areas (e.g. desertification area—HEIFE) and high elevation areas (e.g. Tibetan Plateau) with an inhomogeneous landscape are characterized by extreme gradients in land surface properties, such as wetness, roughness and temperature, which have a significant but local impact on the atmospheric boundary layer (ABL). Observations of the actual extent over these areas are essential to understanding the mechanisms through which inhomogeneous land surfaces may have a significant impact on the structure and dynamics of the overlying ABL. Progress in this research area requires spatial measurements of variables such as surface hemispherical reflectance, radiometric surface temperature, Normalized Difference Vegetation Index (NDVI), Modified Soil Adjusted Vegetation Index (MSAVI), vegetation coverage, leaf area index (LAI), local aerodynamic roughness length, etc. Imaging radiometric on board satellites can provide useful estimates of most of these variables. By using these variables we can derive the distributions of land surface heat fluxes over inhomogeneous landscape.

Parameterization method to derive the regional land surface variables, vegetation variables and land surface heat fluxes over inhomogeneous landscape by using NOAA AVHRR data and field observations has been proposed in this book. The method was applied to the GAME/Tibet area. The distributions and seasonal variations of NDVI, MSAVI, vegetation coverage, leaf area index (LAI), surface reflectance, surface temperature, net radiation flux, soil heat flux, sensible heat flux and latent heat flux have been determined over the GAME/Tibet area. The derived results have been validated by using the “ground truth”, and this implies that the derived results are acceptable.

New parameterization methods to derive the regional land surface variables, vegetation variables and land surface heat fluxes over inhomogeneous landscape by combining Landsat TM data and field observations have also been proposed in this book. The methods were applied to the inhomogeneous areas of HEIFE and AECMP'95. The distributions of NDVI, MSAVI, vegetation coverage, leaf area index (LAI), surface reflectance, surface temperature, net radiation flux, soil heat flux, sensible heat flux and latent heat flux have been determined over these two areas. By using the “ground truth” we validated the derived results. A comparison between the former results (of which the land surface variables and surface heat fluxes were derived from Surface Energy Balance Algorithm for Land—SEBAL) and the results derived from new parameterization method has also been given in this book. The results show that the new satellite remote sensing

List of tables

Tables

Table 1.1	Major land surface processes experiments (LSPE) in the world (1986–2000)	3
Table 2.1	The collected field data of GAME/Tibet(May 10–September 10, 1998)	14
Table 2.2	The collected field data of HEIFE.....	17
Table 2.3	The collected field data of AECMP'95 (August 7–August 21, 1995)	19
Table 3.1	Aerodynamic roughness length z_{0m} derived from different land surfaces by using the independent method	38
Table 3.2	Thermodynamic roughness z_{0h} derived from different land surfaces	39
Table 3.3.	Excess resistance to heat transfer kB^{-1} derived from different land surfaces	40
Table 4.1	Split-Window Algorithms	60
Table 4.2	Examples of effective roughness studies based on different approaches	70
Table 4.3	Typical values for aerodynamic roughness length over homogeneous surfaces and heterogeneous landscape	72
Table 4.4	Some practical equations on kB^{-1}	73
Table 4.5	Comparison of measured values on the GAME/Tibet site versus those derived from remote sensing retrieval method with MAPD	77
Table 5.1	The values of a_1 and a_2 for TM data	84
Table 5.2	The comparison of the value of land surface variables and net radiation obtained from field observation and by TM over HEIFE area.	102
Table 5.3	The comparison of the value of sensible and latent heat flux obtained from field observation and by TM at HEIFE station (Linze —oasis)	102
Table 6.1	The mean absolute percent difference (MAPD) between the derived results and measured values on the HEIFE site	123
Table 6.2	The distribution ranges and peaks of land surface variables, vegetation variables and land surface heat fluxes over HEIFE area.	126
Table 6.3	The distribution ranges and peaks of land surface variables, vegetation variables and land surface heat fluxes over AECMP'95 area	129